**Preparation of thick dense ceramic films of dielectric $BaTaO_2N$ through electrophoretic deposition**

**Authors:**

Hiroto Takeuchi[1], Daiki Miyamoto[1], Yuji Masubuchi[2*], Mikio Higuchi[2], Kento Ishii[3], and Tetsuo Uchikoshi[3]

[1]Graduate School of Chemical Sciences and Engineering, Hokkaido University, N13 W8, Kita-ku, Sapporo, 060-8628, Japan

[2]Faculty of Engineering, Hokkaido University, N13 W8, Kita-ku, Sapporo, 060-8628, Japan

[3]Research Center for Functional Materials, National Institute for Materials Science, 1-2-1 Sengen, Tsukuba, 305-0047, Japan

*Corresponding Author: Yuji Masubuchi; address: Faculty of Engineering, Hokkaido University, N13 W8, Kita-ku, Sapporo, 060-8628, Japan; Tel: +81-(0)11-706-6742; e-mail: yuji-mas@eng.hokudai.ac.jp

**Abstract**

Sintering of the ferroelectric perovskite oxynitride, $BaTaO_2N$ is still a big challenge, because

nitrogen is partially released from the crystal lattice during high-temperature sintering. Post-sintering annealing under an $NH_3$ flow is essential in order to compensate for this nitrogen loss and to recover the electrically insulating properties of the ceramic. However, fully densified bulk ceramics are nitrided only on their outer surface, while their interior remains semiconducting. In this work, thick ceramic films of the perovskite oxynitride with a high relative density close to 90% were fabricated using electrophoretic deposition and high-temperature sintering. The nitrogen loss was fully recovered during annealing under an $NH_3$ flow, owing to the thickness of the sintered films being less than 100 μm. After annealing, the $BaTaO_2N$ ceramics consisted of 200 nm-sized particles with a dense microstructure. This is the first report of the fabrication of $BaTaO_2N$ ceramics with a relative density of 89%. The dielectric constant and dielectric loss were approximately 320 and 0.05 at 1 MHz, respectively.

Keywords: A. Sintering; C. Dielectric property; D. Oxynitrides; D. Perovskite

**Introduction**

Perovskite-type oxynitrides have attracted much attention as lead-free dielectric materials [1-3]. Their ferroelectric behavior has been reported to result from local *cis*-type O/N ordering in the perovskite structures [4-7]. Sintering of perovskite-type oxynitrides has been performed to

investigate their dielectric properties without electrical current leakage [8-10]. However, the preparation of dense ceramics of these oxynitrides is still a big challenge because nitrogen is partially released at sintering temperatures above 900 and 950 °C for $BaTaO_2N$ and $SrTaO_2N$ perovskites, respectively, even under a $N_2$ atmosphere [11]. After sintering, annealing under an $NH_3$ flow is crucial for preparing electrically insulating bulk ceramics with a stoichiometric O/N content. To achieve nitridation of the interior of these bulk ceramics, the relative density (RD) was limited to approximately 80%. Poorly sintered ceramics allow the diffusion of ammonia gas into the interior. Dielectric constants with small temperature dependencies were measured for $BaTaO_2N$ and $SrTaO_2N$ ceramics with an RD of 73% and 83%, respectively [8,9]. However, highly densified ceramics with no nitrogen deficiency are required for practical applications as dielectric materials.

To suppress nitrogen release, low-temperature sintering of $BaTaO_2N$ with a coexisting $BaCN_2$ melt was performed at 910 °C using spark plasma sintering (SPS) [12]. Bulk $BaTaO_2N$ ceramics with an RD of 84% obtained without $NH_3$ annealing have been reported [12]. SPS was also applied to the perovskite $LaTiO_2N$, and an RD as high as 94% was achieved by high-temperature sintering at 1350 °C for a short duration. The resulting sintered ceramic was a perovskite oxynitride contaminated with a non-negligible amount of electrically conducting impurities [13].

Dense $BaTaO_2N$ and $SrTaO_2N$ ceramics with RD > 90% were obtained above 1400 °C in a $N_2$ atmosphere, but could only be nitrided in a thin surface layer with a thickness of approximately 10

μm [14,15]. The thin surface layer recovered its nitrogen content and electrically insulating behavior after annealing in $NH_3$, although the interior of the ceramic remained electrically conducting [14,15]. Thick films of dense oxynitride perovskite ceramics with several tens of micrometers in thickness are expected to enable both a high RD and full nitridation even after annealing in $NH_3$.

Electrophoretic deposition (EPD) is useful for fabricating thin films of ceramic powder compacts from a colloidal suspension [16,17]. The thickness and microstructure of the powder compacts can be controlled by varying the deposition conditions, such as the suspension concentration, deposition time, and applied voltage. The EPD process has been widely employed to fabricate photocatalytic electrodes from fine powders of oxynitride perovskites [18-20]. Oxynitride electrodes prepared by EPD have a porous structure with a thickness of several micrometers. To the best of our knowledge, EPD has not been used to fabricate thick dense films of perovskite oxynitrides to achieve both high RD and electrically insulating behavior after high-temperature sintering and subsequent annealing in $NH_3$.

Among the dielectric perovskite oxynitrides, $BaTaO_2N$ is expected to show the highest dielectric constant [8-10]. In the present study, EPD was used for the first time to fabricate thick powder compacts of the perovskite-type oxynitride $BaTaO_2N$, which were then sintered to form dense $BaTaO_2N$ ceramics with nitrogen deficiency. The ceramics could be fully nitrided by subsequent nitridation in $NH_3$ to recover the electrically insulating properties. Dense $BaTaO_2N$ ceramics with an

RD close to 90% were obtained in thick-film form (~100 μm), and showed larger dielectric constants and lower dielectric loss than previous bulk ceramics having a lower RD.

**Experimental procedure**

$BaTaO_2N$ powders were prepared by an ammonolysis reaction of a mixture of $BaCO_3$ (Fuji Film Wako Pure Chemicals, 99.9%) and $Ta_2O_5$ (Fuji Film Wako Pure Chemicals, 99.9%) with a Ba:Ta molar ratio of 1.03:1. The powder mixture was placed on an alumina boat and loaded in a quartz tube furnace. The sample was heated at 950 °C for 45 h under a 100 mL/min $NH_3$ flow with intermittent grinding runs, similarly to the procedure described in our previous paper [9]. The Ba-rich starting composition was crucial for preparing single-phase $BaTaO_2N$ perovskite oxynitride by the nitridation reaction.

Powder compacts having a thickness of approximately 100 μm were fabricated from a mixture of $BaTaO_2N$ and a $BaCO_3$ additive using the EPD method. The $BaCO_3$ additive compensated for the small amount of Ba loss that occurs during high-temperature sintering [9]. Isopropyl alcohol (IPA; Nacalai Tesque, Inc. 99.7%) and polyethyleneimine (PEI; Fuji Film Wako Pure Chemicals, MW 10000) were used as a dispersion solvent and dispersing agent, respectively, to prepare stable colloidal solutions. The IPA was dehydrated by molecular sieves before use. 1.2 g of $BaTaO_2N$ and $BaCO_3$ were each dispersed in 40 mL of IPA. After adding the PEI, the colloidal solutions were

homogenized by ball milling with zirconia balls for 12 h. The zeta potential for each colloidal suspension was tuned to +40 mV by changing the amount of PEI. The $BaTaO_2N$ and $BaCO_3$ colloidal solutions were mixed at a ratio of 2.5 wt% of $BaCO_3$ in $BaTaO_2N$. A carbon-coated glass substrate was used as an anode and a stainless steel (SUS) plate was the counter electrode. The EPD process was conducted at 50 V for 3-5 min with a 5 mm distance between the electrodes. The deposited powder compacts had a thickness of approximately 100 μm after drying.

After drying under ambient conditions, thick films of the powder compacts were peeled off from the substrate and were sintered at 1380, 1400 and 1420 °C for 4 and 8 h in a $N_2$ atmosphere at 0.2 MPa pressure. The powder compacts were placed in an alumina crucible with/without a small amount of $B_2O_3$ powder additive, which was separated from the compacts. $B_2O_3$ has been reported as a sintering aid together with $SrCO_3$ for $SrTaO_2N$ to form a Sr-B-O liquid phase during sintering [21]. The effect of the $B_2O_3$ additive on the sintering of $BaTaO_2N/BaCO_3$ was also investigated in this study by supplying $B_2O_3$ to the powder compacts via the vapor phase. The sintered thick films of $BaTaO_2N$ became black in color and electrically conducting owing to nitrogen loss during high-temperature sintering. To recover the nitrogen content and electrically insulating properties, the sintered ceramics were subsequently annealed at 950 °C for 100 h in a $NH_3$ flow at 100 mL/min. The powder and sintered products were characterized by X-ray diffraction (XRD) using a Rigaku Ultima-IV diffractometer with Cu Kα radiation operated at 40 kV and 40 mA. XRD patterns were

obtained in the angular range of 2θ=20-90° with a scanning speed and step size of 10°/min and 0.02°, respectively. The zeta potential for the colloidal solutions was measured by a zeta-potential analyzer (Zetasizer Nano-Z, Malvern Panalytical). The microstructure of the powders and sintered ceramics was observed using scanning electron microscopy (SEM; JSM-6500F and JSM-6390LV, Jeol). The particle sizes of the precursors and the ceramics were determined by examining more than 100 grains in the SEM images. Optical images of the powder compacts and sintered ceramics were obtained using an optical microscope (VHX-2000, KEYENCE). The RD was measured using the geometric size and weight of the ceramics. The Ba to Ta ratios in the sintered products were analyzed using X-ray fluorescence spectroscopy (XRF; SEA6000VX-SII, Hitachi). The dielectric properties of the post-annealed samples were measured at room temperature in the frequency range of 120 Hz – 1 MHz using an AC impedance analyzer (IM3536, HIOKI). Pt electrodes were deposited on both sides of the ceramics by sputtering.

**Results and discussion**

Single-phase cubic perovskite $BaTaO_2N$ was obtained by an ammonolysis reaction of the $BaCO_3$ and $Ta_2O_5$ mixture as shown in Fig. 1. The cubic lattice parameter was 0.41134(3) nm, which is consistent with the literature value, $a$ = 0.41128 nm [22]. The morphologies of the powder samples, $BaTaO_2N$ and $BaCO_3$ additive were observed using SEM. The average particle size of $BaTaO_2N$ was

approximately 100 nm, and the particles agglomerated to form micrometer-sized secondary grains as shown in Fig. 2(a). Fig. 2(b) shows $BaCO_3$ particles having an ellipsoidal morphology with short and long axes of approximately 90 and 250 nm, respectively.

Colloidal suspensions were prepared in IPA for each oxynitride and carbonate powder. To prepare stable colloidal suspensions and achieve homogeneous mixing of the two suspensions containing $BaTaO_2N$ and the $BaCO_3$ additive, the zeta potential for each suspension was adjusted prior to the EPD process. The addition of PEI as a dispersing agent increased the zeta potential, and an almost constant value about +40 mV was obtained at 24 mg of PEI for $BaTaO_2N$ and $BaCO_3$ in each 40 mL IPA suspension. After mixing the colloidal suspensions, EPD was performed at an applied voltage of 50 V between the electrodes with a gap of 5 mm. A carbon-coated glass substrate was placed on the anode, and the cathode electrode was a SUS plate. Films with a thickness of approximately 100 μm were formed after a deposition time of roughly 3-5 min as shown in Fig. 2(c). Fig. 2(d) shows an SEM image of a deposited powder compact formed from homogeneously dispersed starting powders. The RD for the powder compact was 43%. The homogeneous distribution of $BaCO_3$ in $BaTaO_2N$ was confirmed by the SEM-EDS elemental mapping image shown in Fig. S1 of the Supporting Information.

The $BaTaO_2N$ thick-film powder compact was sintered at 1400 °C for 4 h under a $N_2$ atmosphere with and without the $B_2O_3$ additive. XRD patterns for the sintered products are shown in Fig. 3.

After high-temperature sintering under a $N_2$ atmosphere, the color of the thick films changed from red to black, indicating partial nitrogen loss from the perovskite lattice. A single-phase perovskite structure was observed for the sintered ceramic prepared without using $B_2O_3$, and a tiny amount of secondary phases appeared for the product sintered with the $B_2O_3$ additive (Fig. 3). The $B_2O_3$ reacted with a small amount of Ba in the powder compact and Ta-rich secondary phases appeared in the sintered ceramic, as previously observed for sintering of $SrTaO_2N$ with a $B_2O_3$ additive [21]. The SEM images of the fracture surfaces of the sintered ceramics show a dense microstructure for the product sintered with $B_2O_3$ (Fig. 4(a)). On the other hand, the ceramics sintered without $B_2O_3$ were porous (Fig. 4(b)), but the grain size was larger than in those sintered with $B_2O_3$. The RD values were 92% and 78% for $BaTaO_2N$ sintered with and without $B_2O_3$, respectively. The improvement in sinterability brought about by $B_2O_3$ was studied for the sintering of $SrTaO_2N$ with the $B_2O_3$ additive, which formed a strontium borate amorphous grain boundary phase having a low melting temperature [23]. In the present study, a Ba-B-O liquid phase improved the densification of the oxynitride grains, and an RD value above 90% was achieved. The smaller grains obtained by sintering with $B_2O_3$ could be explained by the occurrence of sintering with a small amount of liquid phase for a short duration, before reaching the grain-growth-dominant step in the liquid-phase sintering process. By increasing the sintering time from 4 to 8 h, grains larger than 1 μm were formed, similar to the case of sintering at 1420 °C, as discussed below. On the other hand, sintering without $B_2O_3$ corresponded to solid-

phase sintering, and grain growth was accelerated by nitrogen deficiency, resulting in large grains. The $B_2O_3$ additive improved the sintering of $BaTaO_2N$, similar to the case for $SrTaO_2N$, although the optimum amount of $B_2O_3$ for liquid-phase sintering needs to be further investigated in future work. The sintering temperature and time were further investigated to improve the microstructure of the films sintered with the $B_2O_3$ additive. SEM images of the fracture surfaces of the sintered ceramics are shown in Fig. 5. A porous morphology is observed for the product sintered at 1380 °C for 4 h (Fig. 5(a)). A dense structure consisting of grains with an average sizes of 200 nm was obtained after sintering at 1400 °C for 4 h. Inhomogeneous grain growth was observed for the products sintered at 1400 °C for 8 h and 1420 °C for 4h, and micrometer-scale grains appeared as shown in Figs. 5(c,d). The RD values for the sintered ceramics before annealing were 85, 92, 88 and 89% for ceramics sintered at 1380 °C for 4 h, 1400 °C for 4 h, 1400 °C for 8 h, and 1420 °C for 8 h, respectively. The $B_2O_3$ additive is expected to form a liquid phase at around 1400 °C, and the Ba-rich region in the $BaO$-$B_2O_3$ system has a maximum melting temperature of 1372 °C [24]. At 1380 °C, the amount of liquid phase may be less than that required for complete coverage of the oxynitride grains. On the other hand, a higher sintering temperature or prolonged sintering may promote inhomogeneous grain growth.

The thick ceramic film sintered at 1400 °C for 4 h with the $B_2O_3$ additive was annealed in a $NH_3$ flow at 950 °C for a long duration to compensate for the nitrogen deficiency that developed during

high-temperature sintering. The sample color gradually changed from black to red with increasing annealing time and the nitrided area extended from the outer surface to the interior as shown in Fig. 6. Full nitridation was confirmed by the red color of the sintered product after annealing for 100 h, as shown in Fig. 6(d); this color was almost the same as that for powder compact (Fig. 6(a)). Recovery to single-phase $BaTaO_2N$ perovskite was also verified by the XRD pattern shown in Fig. 7. A small amount of a Ba-rich tantalum oxide appeared in the sintered ceramics, along with a TaN secondary phase with a rock-salt-type structure. These impurity phases were negligible after post-annealing in $NH_3$ at 950 °C for 100 h. The lattice parameter for the perovskite phase was 0.431139(1) nm after annealing, i.e., slightly larger than the value of 0.41100(1) nm for N-deficient $BaTaO_2N$ ceramics before annealing [9]. The Ba/Ta ratio in the annealed product was 50.6/49.4 as measured by XRF. The slightly Ba-rich composition corresponds to a small amount of Ba-B-O phase, which formed during the sintering with $B_2O_3$ and 2.5 wt% $BaCO_3$, coexisting in the perovskite phase. After nitridation, the RD of the thick ceramics was approximately 89 %, which was slightly lower than that before the annealing step. A slight decrease in RD has also been reported for bulk ceramics of $BaTaO_2N$ and $SrTaO_2N$ after nitridation of black sintered ceramics [8,9]. The SEM images show that the morphology of $BaTaO_2N$ did not change dramatically upon annealing in flowing $NH_3$, as shown in Fig. 5(e).

After annealing for 100 h, full nitridation was achieved only for the samples sintered at 1380 and

1400 °C for 4 h, while those sintered at 1420 °C for 4 h and 1400 °C for 8 h were not internally nitrided. The interior of the ceramic was still black in color and many cracks were formed at grain boundaries and transgranular regions, as shown in Fig. 5(f). N-deficient $BaTaO_2N$ has a smaller unit cell volume than stoichiometric $BaTaO_2N$ [9]. Nitridation of N-deficient $BaTaO_2N$ increased the unit cell volume and induced additional stress in the ceramics. Poorly sintered ceramics obtained at 1380 °C can release the stress because of the large amount of free space, which can accommodate the lattice expansion. Dense ceramics sintered at 1400 °C for 4 h kept their microstructure during the nitridation process (Fig. 5(e)). The ceramic consisting of smaller grains sustained additional stress induced by unit cell expansion. The fracture toughness depends on the grain size, a smaller grain size being associated with higher toughness [25-27]. On the other hand, sintering at 1420 °C or for a long duration dramatically enhanced grain growth, as shown in Figs. 5(c,d). Nitridation caused fracture of the ceramics at grain boundaries and in transgranular regions (Fig. 5(f)). In polycrystalline ceramics, formation of larger particles reduces the grain boundary area and facilitates propagation of cracks through the grains. Fabrication of dense ceramics consisting of finer grains at 1400 °C for 4 h was pivotal for the $BaTaO_2N$ to maintain a dense microstructure during annealing in $NH_3$ and to recover its electrically insulating properties. Sintering at 1400 °C for 4 h formed a suitable amount of liquid phase, which densified the powder compact while keeping the particle size smaller.

The dielectric properties of the $BaTaO_2N$ ceramics sintered at 1400 °C for 4 h after nitridations at

950 °C for 0, 60 and 100 h are shown in Fig. 8. N-deficient $BaTaO_2N$ ceramics without a subsequent nitridation treatment show large dielectric constants above 30000 with large dielectric loss values of 0.6-1. Both the large dielectric constant and dielectric loss can be explained by the semiconducting nature of the black sintered ceramic. After nitridation for 60 h, only the surface part of the thick ceramic was nitrided, recovering its original red color, as shown in Fig. 6(c). The dielectric constant decreased to several hundred, and the dielectric loss also decreased but was above 0.1. In previous research, the large dielectric constant was found to originate from residual semiconducting regions, which was not fully nitrided due to the dense bulk structure [8]. The fully nitrided sample with a red interior obtained in this study, as shown in Fig. 6(d), exhibited dielectric constants of 530-320 at 120-$10^6$ Hz with tanδ values of 0.15-0.05, respectively. These dielectric constants were larger than, and the dielectric losses were lower than, those for previous bulk ceramics ($\varepsilon_r$ = 300 and tanδ = 0.06 at $10^5$ Hz) with an RD of 73%. The larger dielectric constants for the $BaTaO_2N$ ceramic films were attributed to the higher RD value for the fully nitrided thick ceramic film. The bulk ceramic with an RD of 73% was nitrided owing to its porous structure, but some residual semiconducting nature might remain after the short nitridation run. In this study, the use of a thick ceramic film significantly enhanced the subsequent nitridation reaction because the thickness was 100 μm and the nitridation period was as long as 100 h. Full recovery of the chemical composition eliminated the residual semiconducting behavior and improved the insulating nature of the films.

## Conclusion

A post-sintering nitridation process is essential for obtaining highly insulating ceramics of $BaTaO_2N$ perovskite. However, the nitridation reaction is difficult for dense bulk ceramics. In the present study, a thick $BaTaO_2N$ film with an RD of 89% that exhibited full recovery of electrically insulating behavior was fabricated by the EPD process and high-temperature sintering with a $B_2O_3$ additive, followed by annealing in $NH_3$. The $B_2O_3$ additive improved the densification of the $BaTaO_2N$ ceramic and formed a homogeneous fine-grained structure upon sintering at 1400 °C for 4 h. A large dielectric constant of 320 and a low dielectric loss of 0.05 at 1 MHz were achieved for dense $BaTaO_2N$ ceramics after nitridation for 100 h. The sintered ceramics with a thickness of 100 μm consisted of relatively small grains, which is important for obtaining insulating $BaTaO_2N$ while keeping the dense structure after the nitridation reaction.

## Acknowledgement

This work was supported in part by the NIMS Joint Research Hub Program. A part of this research was conducted at “Joint-use Facilities: Laboratory of Nano-Micro Material Analysis”, Hokkaido University, supported by “Advanced Research Infrastructure for Materials and Nanotechnology in Japan (ARIM)” of the Ministry of Education, Culture, Sports, Science and Technology (MEXT).

Proposal Number JPMXP1222HK0014.

**References**

[1] Y.-I. Kim, R. M. Woodward, K. Z. Baba-Kishi, C. W. Tai, Characterization of the structural, optical, and dielectric properties of oxynitride perovskites $AMO_2N$ (A = Ba, Sr, Ca; M = Ta, Nb), Chem. Mater. 16 (2004) 1267–1276.

[2] Y. Masubuchi, S.-K. Sun, S. Kikkawa, Processing of dielectric oxynitride perovskites for powders, ceramics, compacts and thin films, Dalton Trans. 44 (2015) 10570-10581.

[3] A. Ziani, C. Le Paven-Thivet, D. Fasquelle, L. Le Gendr, R. Benzerga, F. Tessier, F. Chevire, J. C. Carru, A. Sharaiha, Dielectric oxynitride $LaTiO_xN_y$ thin films deposited by reactive radio-frequency sputtering. Thin Solid Films 520 (2012) 4536-4540.

[4] A. Hosono, Y. Masubuchi, S. Yasui, M. Takesada, T. Endo, M. Higuchi, M. Itoh, S. Kikkawa, Ferroelectric $BaTaO_2N$ Crystals Grown in a $BaCN_2$ Flux. Inorg. Chem. 58 (2019) 16752–16760.

[5] Y.-R. Zhang, T. Motohashi, Y. Masubuchi, S. Kikkawa, Local anionic ordering and anisotropic

displacement in dielectric perovskite $SrTaO_2N$. J. Ceram. Soc. Jpn. 119 (2011) 581-586.

[6] Y. Hinuma, H. Moriwake, Y.-R. Zhang, T. Motohashi, S. Kikkawa, I. Tanaka, First-principles study on relaxor-type ferroelectric behavior without chemical inhomogeneity in $BaTaO_2N$ and $SrTaO_2N$. Chem. Mater. 24 (2012) 4343-4349.

[7] H. Wolff, R. Dronskowski, First-principles and molecular-dynamics study of structure and bonding in perovskite-type oxynitrides $ABO_2N$ ($A$ = Ca, Sr, Ba; $B$ = Ta, Nb). J. Comput. Chem. 29 (2008) 2260-2267.

[8] S.-K. Sun, Y.-R. Zhang, Y. Masubuchi, T. Motohashi, S. Kikkawa, Additive sintering, postannealing, and dielectric properties of $SrTaO_2N$. J. Am. Ceram. Soc. 97 (2014) 1023-1027.

[9] A. Hosono, S.-K. Sun, Y. Masubuchi, S. Kikkawa, Additive sintering and post-ammonolysis of dielectric $BaTaO_2N$ oxynitride perovskite. J. Eur. Ceram. Soc. 36 (2016) 3341-3345.

[10] A. Castets, I. Fina, J. R. Guarin, J. Oro-Sole, C. Frontera, C. Ritter, J. Fontcuberta, A. Fuertes, High-temperature synthesis and dielectric properties of $LaTaON_2$. Inorg. Chem. 60 (2021) 16484–

16491.

[11] D. Chen, D. Habu, Y. Masubuchi, S. Torii, T. Kamiyama, S. Kikkawa, Partial nitrogen loss in $SrTaO_2N$ and $LaTiO_2N$ oxynitride perovskites. Solid State Sci. 54 (2016) 2-6.

[12] A. Hosono, M. Inoguchi, Y. Masubuchi, K. Murayama, M. Iha, M. Higuchi, S. Kikkawa, Spark plasma sintering of dielectric $BaTaO_2N$ close to the melting point of the $BaCN_2$ additive. J. Eur. Ceram. Soc. 40 (2020) 2317-2322.

[13] D. Li, W. Li, C. Fasel, J. Shen, R. Riedel, Sinterability of the oxynitride $LaTiO_2N$ with perovskite-type structure. J. Alloys Compd. 586 (2014) 567-573.

[14] S. Kikkawa, S.-K. Sun, Y. Masubuchi, Y. Nagamine, T. Shibahara, Ferroelectric response induced in *cis*-type anion ordered $SrTaO_2N$ oxynitride perovskite. Chem. Mater. 28 (2016) 1312-1317.

[15] A. Hosono, Y. Masubuchi, Y. Nagamine, T. Shibahara, S. Kikkawa, Piezoresponse and microstructure of $BaTaO_2N$ ceramics. J. Eur. Ceram. Soc. 38 (2018) 3478-3482.

[16] P. Sarkar, P. S. Nicholson, Electrophoretic deposition (EPD): mechanisms, kinetics, and application to ceramics. J. Am. Ceram. Soc. 79 (1996) 1987-2002.

[17] F. Tang, T. Uchikoshi, K. Ozawa, Y. Sakka, Effect of polyethyleneimine on the dispersion and electrophoretic deposition of nano-sized titania aqueous suspensions. J. Eur. Ceram. Soc. 26 (2006) 1555-1560.

[18] K. Maeda, M. Higashi, B. Siritanaratkul, R. Abe, K. Domen, $SrNbO_2N$ as a water-splitting photoanode with a wide visible-light absorption band. J. Am. Chem. Soc. 133 (2011) 12334-12337.

[19] L. Zhang, Y. Song, J. Feng, T. Fang, Y. Zhong, Z. Li, Z. Zou, Photoelectrochemical water oxidation of $LaTaON_2$ under visible-light irradiation. Int. J. Hydrog. Energy. 39 (2014) 7697-7704.

[20] B. Dong, Y. Qi, J. Cui, B. Liu, F. Xiong, X. Jiang, Z. Li, Y. Xiao, F. Zhang, C. Li, Synthesis of $BaTaO_2N$ oxynitride from Ba-rich oxide precursor for construction of visible-light-driven Z-scheme overall water splitting. Dalton Trans. 46 (2017) 10707-10713.

[21] Y. Masubuchi, D. Miyamoto, M. Higuchi, $B_2O_3$ as a new sintering additive for perovskite type $SrTaO_2N$ oxynitride ceramics. J. Asian Ceram. Soc. 10 (2022) 158-164.

[22] F. Pors, R. Marchand, Y. Laurent, P. Bacher, G. Roult, Structural study of $BaTaO_2N$ and $BaNbO_2N$ oxynitride perovskites. Mater. Res. Bull. 23 (1988) 1447-1450.

[23] X. M. Pan, C. Wang, Z. P. Jin, Assessment of the thermodynamics and phase diagram of the SrO-$B_2O_3$ system. Z. Metallkd. 95 (2004) 40-44.

[24] H. Yu, Q. Chen, Z. Jin, Thermodynamic reassessment of the BaO-$B_2O_3$ system. J. Phase Equilib. 20 (1999) 479-484.

[25] T. Tani, Y. Miyamoto, M Koizumi, Grain size dependence of Vickers microhardness and fracture toughness in $Al_2O_3$ and $Y_2O_3$ ceramics. Ceram. Int. 12 (1986) 33-37.

[26] M. Michalek, J. Sedlacek, M. Parchoviansky, M. Michalkova, D. Galusek, Mechanical properties and electrical conductivity of alumina/MWCNT and alumina/zirconia/MWCNT composites. Ceram. Int. 40 (2014) 1289-1295.

[27] T. K. Roy, Assessing hardness and fracture toughness in sintered zinc oxide ceramics through indentation technique. Mater. Sci. Eng. A 640 (2015) 267-274.

**Figure captions**

Fig. 1. XRD pattern for $BaTaO_2N$ precursor powder.

Fig. 2. SEM images of (a) $BaTaO_2N$ and (b) $BaCO_3$ powders, and (c) optical image and (d) SEM image of fracture surface of powder compact after EPD process.

Fig. 3. XRD patterns for $BaTaO_2N$ ceramics sintered (a) with $B_2O_3$ and (b) without $B_2O_3$.

Fig. 4. SEM images of fracture surfaces of $BaTaO_2N$ ceramics sintered at 1400 °C for 4 h (a) with $B_2O_3$ and (b) without $B_2O_3$.

Fig. 5. SEM images of $BaTaO_2N$ ceramics sintered at (a) 1380 °C for 4 h, (b) 1400 °C for 4 h, (c) 1400 °C for 8 h, and (d) 1420 °C for 4 h with $B_2O_3$, and products post-annealed at (e) 1400 °C and (f) 1420 °C for 4 h.

Fig. 6. Optical images of (a) $BaTaO_2N$ powder compact with $B_2O_3$, and ceramics after annealing for (b) 0 h, (c) 60 h, and (d) 100 h.

Fig. 7. XRD patterns for (a) $BaTaO_2N$ ceramics sintered at 1400 °C for 4 h and (b) annealed products.

Fig. 8 Frequency dependence of dielectric constant, $\varepsilon_r$, and dielectric loss, $\tan\delta$, for ceramics sintered at 1400 °C and annealed at 950 °C.

Figure 1

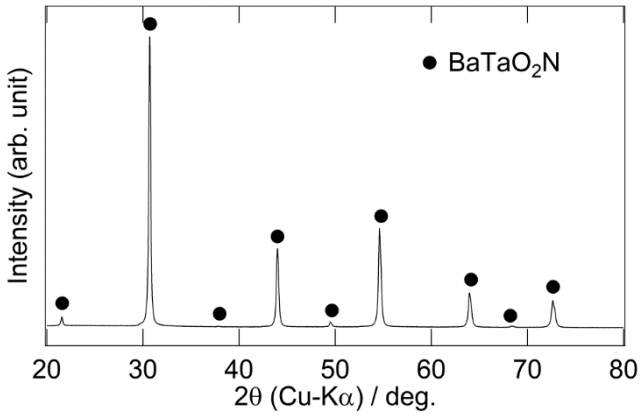

Figure 2

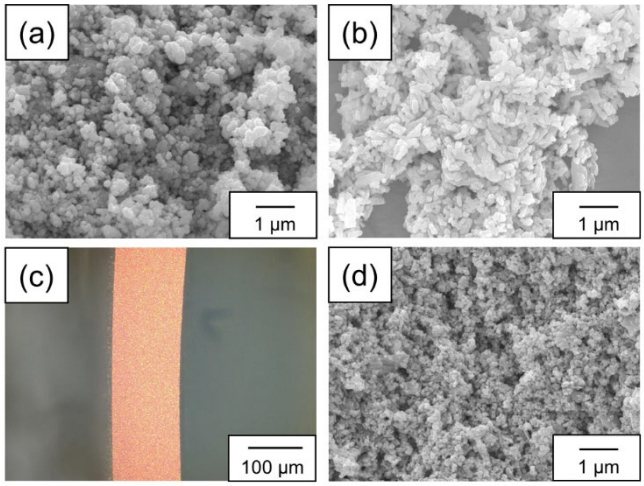

Figure 3

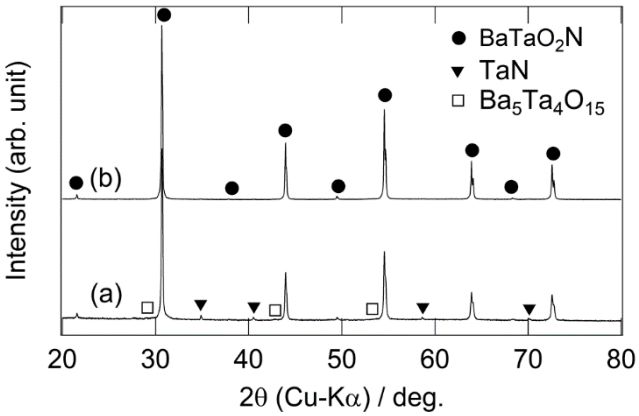
Intensity (arb. unit)
BaTaO2N
TaN
Ba5Ta4O15
(b)
(a)
20
30
40
50
60
70
80
2θ (Cu-Kα) / deg.

Figure 4

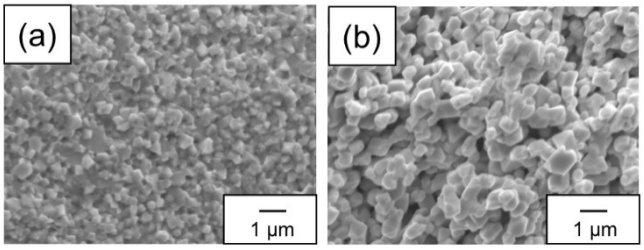

Figure 5

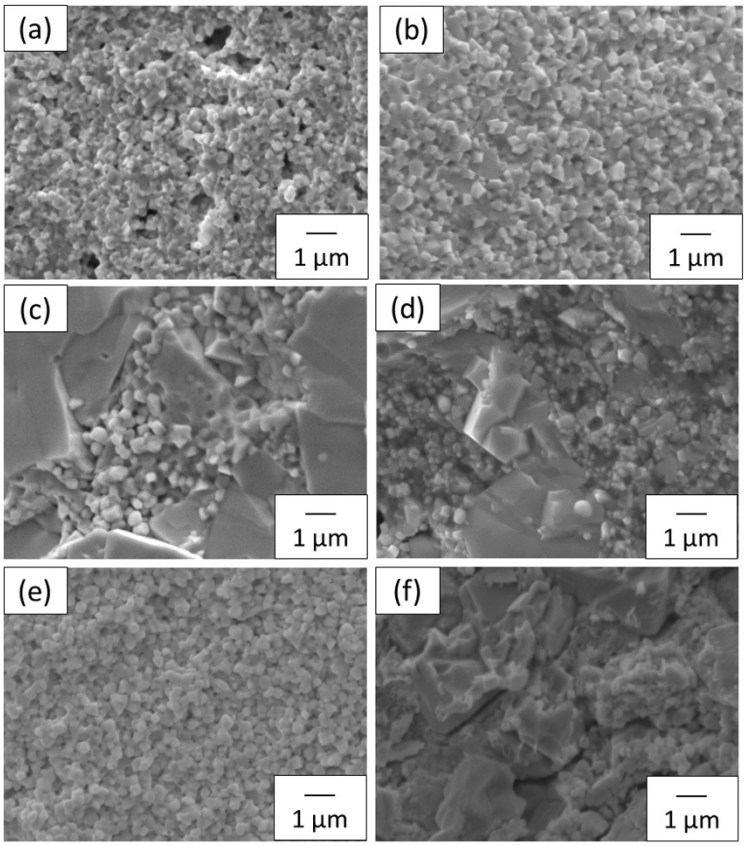

Figure 6

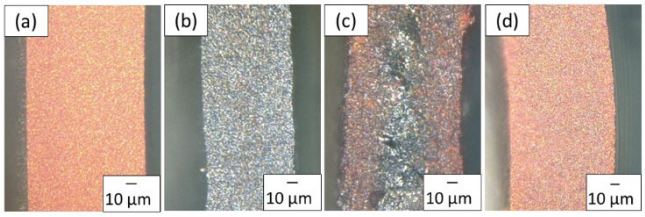

Figure 7

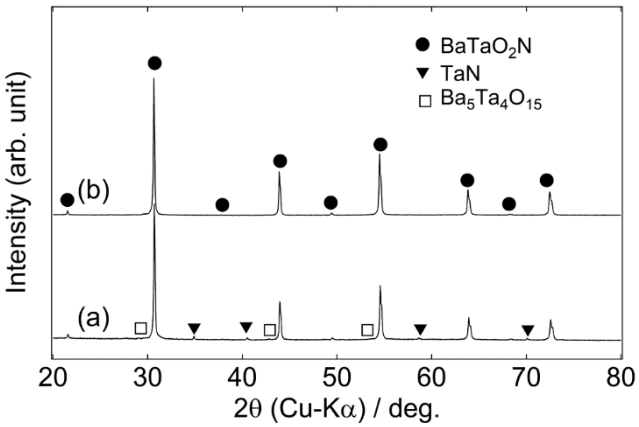
BaTaO2N
TaN
Ba5Ta4O15
(b)
(a)
Intensity (arb. unit)
20
30
40
50
60
70
80
2θ (Cu-Kα) / deg.

Figure 8

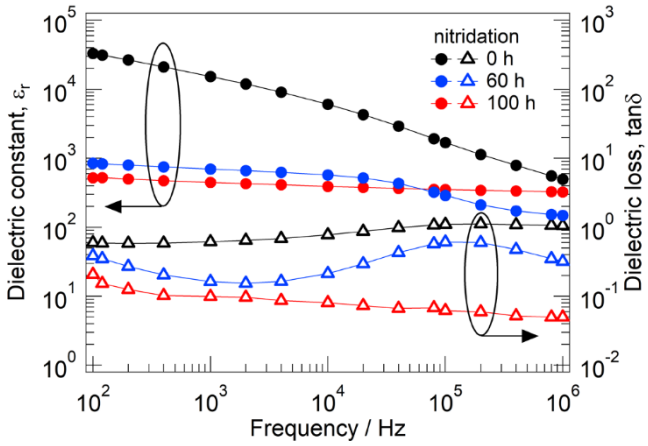
nitridation
0 h
60 h
100 h
Dielectric constant, $\varepsilon_r$
Dielectric loss, tanδ
Frequency / Hz
$10^0$
$10^1$
$10^2$
$10^3$
$10^4$
$10^5$
$10^6$
$10^{-2}$
$10^{-1}$